J Shoulder Elbow Surg (2021) 30, 512–519

ELSEVIER

Journal of Shoulder and Elbow Surgery

www.elsevier.com/locate/ymse

Medial elbow exposure: an anatomic comparison of 5 approaches

Adrian L. Huang, MBBCh BAO, FRCSC[a,*], Michael Hackl, MD[b], Andrea H.W. Chan, HBSc, MA, MD, FRCSC[c], David T. Axford, BESc[c], George S. Athwal, MD, FRCSC[c], Graham J.W. King, MD, MSc, FRCSC[c]

[a]*St. Paul's Hospital Department of Orthopaedic Surgery, University of British Columbia, Vancouver, BC, Canada*
[b]*Department of Orthopedic and Trauma Surgery, University Medical Center of Cologne, Cologne, Germany*
[c]*Hand and Upper Limb Centre, Western University, London, ON, Canada*

Purpose: Several surgical approaches to the medial elbow are described; however, it remains unclear which exposure provides the optimal view of relevant medial elbow structures. The purpose of this anatomic study was to determine the visible surface area of the coronoid process, distal humerus, and radial head through 5 approaches to the medial elbow.

Methods: Eight fresh-frozen cadaveric upper extremity specimens were dissected. Five surgical approaches were performed on each specimen. The Smith muscle-splitting approach to the ulnar collateral ligament was performed first (Smith), followed by the Hotchkiss medial ''Over the top'' approach (Hotchkiss), the extended medial elbow approach (EMEA), the flexor carpi ulnaris splitting approach (FCU-Split), and the Taylor and Scham approach (T&S). Bony visualization was determined using laser surface scanning (Artec Space Spider; Artec 3D). The scans were segmented using commercially available digital software (Geomagic Wrap; 3D Systems Corporation), and the surface area visualized was determined. A descriptive analysis of the joint areas visible using the medial collateral ligament (MCL) as a clinical landmark was performed.

Results: The EMEA visualized the highest proportion of the total elbow joint from the medial side showing 13.9 ± 6.0 cm^2, or 15% ± 4% of the joint. It also provided the best visualization of the coronoid (3.2 ± 1.7 cm^2 of surface area, or 26% ± 9%) and distal humerus (9.9 ± 4.3 cm^2, or 15% ± 4%). The Hotchkiss approach was best at visualizing the radial head (0.8 ± 0.3 cm^2, or 7% ± 3%). The EMEA, Hotchkiss, and Smith approaches showed primarily the anterior bundle of the MCL, its insertion, and the regions anterior to it, whereas the FCU-Split showed the anterior bundle of the MCL and regions both anterior and posterior to it. The T&S showed primarily the areas posterior to the anterior bundle of the MCL; the anterior regions were not visible. The FCU-Split and the T&S allowed visualization of the posterior bundle of the MCL. The intraclass correlation coefficients (ICCs) for intraobserver reliability were 0.997, 0.992, and 0.974 for the test distal humerus, test coronoid, and test radial head, respectively. The ICCs for interobserver reliability were 0.915 for the test distal humerus, 0.66 for the coronoid, and 0.583 for the radial head.

Conclusion: The EMEA provides the most visualization of the coronoid and distal humerus, whereas the Hotchkiss showed the most radial head. However, these approaches mainly visualize structures anterior to the MCL. If exposure of structures posterior to the MCL is required, the FCU-Split and T&S approaches are more appropriate.

Institutional review board approval was not required for this cadaver anatomy study.

*Reprint requests: Adrian L. Huang, MBBCh BAO, FRCSC, St. Paul's Hospital, Room 339A–1081 Burrard Street, Vancouver, BC, Canada V6Z 1Y6.

E-mail address: adrian.huang@ubc.ca (A.L. Huang).

1058-2746/$ - see front matter
https://doi.org/10.1016/j.jse.2020.06.031

Level of evidence: Anatomic Study; Cadaver Dissection

Keywords: Medial elbow; surgical approaches to the elbow; extended medial elbow approach; Hotchkiss over the top; Taylor and Scham; flexor carpi ulnaris split; medial collateral ligament; coronoid

Many surgical exposures exist for approaching the medial side of the elbow. However, depending on whether an anteriorly or posteriorly centered approach is chosen, only certain portions of major anatomic structures, like the medial collateral ligament (MCL), coronoid, distal humerus, and the radial head, are visible. For example, the medial ''Over the top'' approach described by Hotchkiss et al[3] allows access to the elbow anterior to the MCL, whereas the approach described by Taylor and Scham[13] allows visualization of the anatomic structures posterior to the MCL. As such, the question of which exposure provides the optimal view of the coronoid process, distal humerus, and radial head from the medial side remains. The purpose of this anatomic study was to determine the visible surface area of the coronoid process, distal humerus, and radial head through 5 common approaches to the medial elbow.

Methods

Eight fresh-frozen cadaveric upper extremity specimens (6 females, 2 males) with an average age of 74 and average BMI of 25 (range 18-36) were dissected. All specimens were free from previous elbow surgery. Five surgical approaches were performed on each specimen. The sequence was standardized, moving from least to most invasive. The deep and superficial intervals of the approach were carefully closed using a standardized combination of running and interrupted sutures prior to the next surgical approach being performed. The Smith muscle-splitting approach to the ulnar collateral ligament of the elbow[11] (Smith) was performed first followed by the Hotchkiss medial over-the-top approach[3] (Hotchkiss), the extended medial elbow approach[5] (EMEA), the flexor carpi ulnaris splitting approach[4,5,9,12] (FCU-Split), and the Taylor and Scham approach[13] (T&S). All approaches were performed by 1 upper extremity fellow (A.H.) and 1 shoulder and elbow surgeon (M.H.) under the direction of the senior authors (G.A., G.K.).

Surgical approaches

A posterior skin incision[6] was made and a full-thickness fasciocutaneous medial flap was created. The ulnar nerve was identified proximally at the intermuscular septum and traced to the cubital tunnel and between the 2 heads of the flexor carpi ulnaris (FCU). It was transposed anteriorly for the FCU-Split in this study; however, it may also be left in situ during this approach and retracted posteriorly with the ulnar head of the FCU to improve exposure.[9,12] It was also transposed anteriorly for the T&S approach. Retractor placement was standardized for each approach.

The Smith approach (Fig. 1, *a*)[11] was performed by using the internervous plane between the median and ulnar nerves. This is identified superficially at the raphe between FCU and palmaris longus (PL) and FCU and flexor digitorum superficialis in the deep plane. The raphe was identified 1 cm distal to the insertion of the MCL and split down to the level of the MCL, working

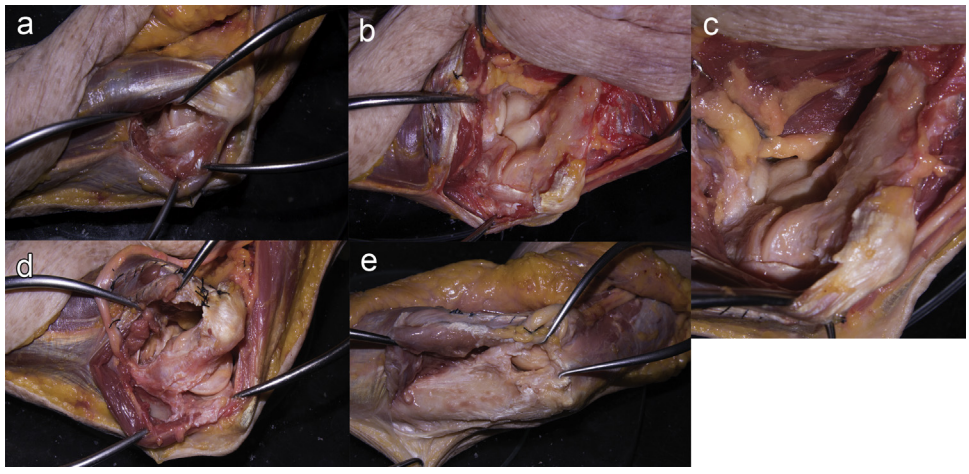

Figure 1 Approaches. (**a**) Smith approach. (**b**) Hotchkiss over-the-top approach. (**c**) Extended medial elbow approach. (**d**) Flexor carpi ulnaris splitting approach. (**e**) Taylor and Scham approach.

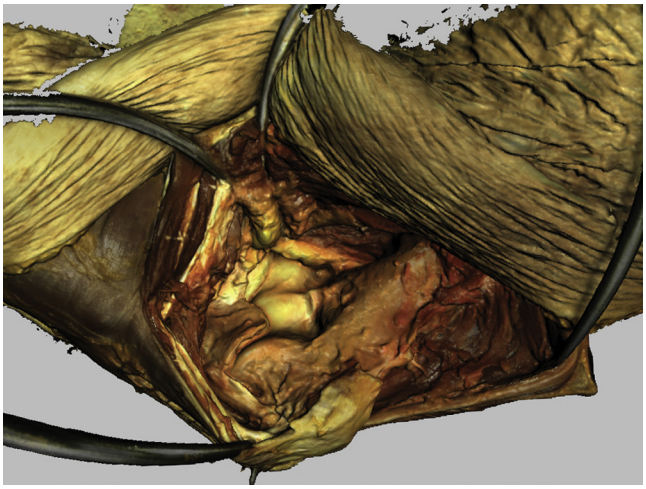

Figure 2 Laser surface scanned specimen.

proximally toward the medial epicondyle. Subperiosteal dissection was performed to access the ulna. The ulnar nerve was retracted with the posterior portion of the FCU.

The Hotchkiss approach[3] (Fig. 1, *b*) was performed by excising the medial intermuscular septum from the supracondylar ridge and then dissecting the brachialis off the anterior humerus. The flexor pronator mass (FPM) was then incised in line with the fibers, leaving 1.5 cm of FCU on the epicondyle. The FPM anterior to this was released, leaving a cuff of tissue on the supracondylar ridge for later repair. An arthrotomy was performed by peeling the capsule off the anterior humerus starting 6 cm proximal to the joint and moving distally.

The EMEA[5] (Fig. 1, *c*) was performed by reopening Smith's interval.[11] The deep dissection was performed in the same manner as the Hotchkiss approach. The flexor digitorum superficialis was lifted, exposing the ulnar head of the pronator teres. The posterior recurrent ulnar artery marked the distal extent of the exposure. The ulnar head of the pronator teres was dissected off the ulna and retracted radially to protect the median nerve. The FCU was lifted off the medial ulna, with the ulnar nerve staying embedded in the mass of the FCU when retracted.

The FCU-Split[4,5,9,12] (Fig. 1, *d*) was performed by following the ulnar nerve down to the split between the 2 heads of the FCU, which was split in line with its fibers until 1 cm distal to the sublime tubercle. The first motor branch of the ulnar nerve was protected while the FPM was retracted anteriorly to expose the sublime tubercle, MCL, and the coronoid. This was done from distal to proximal to better identify the transition of the muscular to fibrous portions of the MCL at the sublime tubercle, better protecting the MCL. Proximally, the FPM was released off the medial epicondyle with a cuff of tissue for repair, for a length of 1 cm to improve visualization. The ulnar head of the FCU was partially elevated from the capsule and ulna and retracted posteriorly. The posterior bundle of the MCL was incised in the floor of the cubital tunnel.

The T&S approach[13] (Fig. 1, *e*) was performed by incising along the triangular subcutaneous area of the ulna and raising the periosteum medially. The muscular origin of the flexor digitorum profundus was elevated, and the ulnar head of the flexor digitorum superficialis and the deep head of the pronator teres were freed. Dissection was carried anteriorly and proximally until the anterior margin of the coronoid and the sublime tubercle were delineated.

Image analysis: bony surface area

Imaging was performed using a laser surface scanning system with digitization (Artec Space Spider and Artec Studio 12; Artec 3D, Santa Clara, CA, USA) (Fig. 2). The radius, ulna, and humerus were then stripped of soft tissue and laser surface scanned in the same manner to serve as control specimens. The scans were then segmented using commercially available software (Geomagic Wrap; 3D Systems Corporation, Rock Hill, SC, USA) and the surface area visualized determined digitally within the same program. The base of the coronoid was defined as a line from the medial and anterior aspect of the bare area connecting to the slope change of the coronoid process, a modification of the method described by Matzon et al,[7] allowing full inclusion of the sublime tubercle (Fig. 3, *a*). The distal humerus was segmented at the level of the proximal extent of the coronoid fossa, with the cut line being perpendicular to the humeral shaft on a medial view of the humerus (Fig. 3, *b*). The radial head was cut at the distal part of the articular cartilage, with the cut line perpendicular to the articular surface of the radial head (Fig. 3, *c*).

Surface area measurements consisted of measuring the absolute value of the surface area visualized and the proportion of the surface area as compared to the corresponding stripped control specimen.

Image analysis: coronoid height and visualization

Coronoid height was defined as a modification of the method described by Matzon et al.[7] A vertical line, originating from the previously described base of the coronoid that intercepted the highest portion of the coronoid, was used as the height (Fig. 4). Height measurements were taken as absolute values and as proportions of the total height.

A descriptive analysis of the joint areas visible was performed using the MCL as a clinical landmark. Regions anterior or posterior to the MCL through each approach were noted.

Statistical analysis

Differences in the absolute surface area visualized of the coronoid, distal humerus and radial head, and the proportion of each as a fraction of the stripped controls, was determined through statistical analysis (SPSS software; IBM Inc., Armonk, NY, USA). The total visible joint, defined as the sum of the surface areas of the coronoid, distal humerus, and radial head, was also measured. A repeated measures analysis of variance was performed with the statistical significance set at $P < .05$. Interobserver reliability was performed by 2 observers (A.H., A.C.). Intraobserver reliability was performed by a single observer (A.H.) repeating the measurements 1 month after taking the original measurements. Intraclass correlation coefficients (ICCs) with a 2-way random effects model and absolute agreement were used.[10] Classifications for ICC results were interpreted according to Shrout[10] and Cicchetti and Sparrow[1] as poor (ICC < 0.40), fair (ICC $= 0.40$-0.59), good (ICC $= 0.60$-0.74), and excellent (ICC > 0.74).

Figure 3 Surface area definitions. (**a**) Coronoid. 1: medial view; 2, lateral view; 3, anterior view. (**b**) Distal Humerus. 1: anterior view; 2, medial view. (**c**) Radial head.

Results

The average total surface area of the stripped controls was 65.4 ± 13.2 cm^2 for the distal humerus, 12.0 ± 2.9 cm^2 for the coronoid, and 11.7 ± 2.6 cm^2 for the radial head.

The EMEA showed the highest proportion of the total elbow joint from the medial side, with a surface area of 13.9 ± 6 cm^2 (Table IA; 15% ± 4% of the joint, Table IIA) (Fig. 5). This was followed by the Hotchkiss (13% ± 3%, $P = .101$), FCU-Split (6% ± 3%, $P < .001$), T&S (4% ± 0.9%, $P < .001$), and Smith (2% ± 1%, $P < .001$) (Table IIA).

The EMEA also showed the highest amount of distal humerus surface area with 9.9 ± 4.3 cm^2 (Table IB; 15% ± 4% by proportion, Table IIB), followed by the Hotchkiss (13% ± 3%, $P = .123$), FCU-Split (6% ± 2%, $P < .001$), T&S (2% ± 1%, $P < .001$), and Smith (2% ± 1%, $P < .001$) (Table IB).

The Hotchkiss showed the highest area and proportion of the radial head, with 0.8 ± 0.3 cm^2 (Table IC) and 7% ± 3% (Table IIC), respectively, followed by the EMEA (0.8 ± 0.3 cm^2, or 7% ± 2%, $P = .887$) and FCU-Split (0.02 ± 0.06 cm^2, or 0.2% ± 1%, $P < .001$) (Table IC and Table IIC). The radial head was not visible with either the T&S or Smith approaches.

Figure 4 Coronoid height.

Table I Surface area of joint anatomy visible

Approach	Visible	Comparison	*P* value
A: Total joint surface area (cm^2)			
EMEA	13.9 ± 6		
		vs. Hotchkiss	.294
		vs. FCU-Split	<.001
		vs. T&S	<.001
		vs. Smith	<.001
Hotchkiss	11.6 ± 5		
		vs. FCU-Split	<.001
		vs. T&S	<.001
		vs. Smith	<.001
FCU-Split	5 ± 2.2		
		vs. T&S	.359
		vs. Smith	.164
T&S	3.1 ± 1.3		
		vs. Smith	.432
Smith	2 ± 0.9		
B: Distal humerus surface area (cm^2)			
EMEA	9.9 ± 4.3		
		vs. Hotchkiss	.330
		vs. FCU-Split	<.001
		vs. T&S	<.001
		vs. Smith	<.001
Hotchkiss	8.5 ± 3.6		
		vs. FCU-Split	<.001
		vs. T&S	<.001
		vs. Smith	<.001
FCU-Split	3.6 ± 1.5		
		vs. T&S	.122
		vs. Smith	.101
T&S	1.4 ± 0.5		
		vs. Smith	.826
Smith	1.1 ± 0.5		
C: Radial head surface area (cm^2)			
Hotchkiss	0.8 ± 0.3		
		vs. EMEA	<.895
		vs. FCU-Split	<.001
EMEA	0.8 ± 0.3		
		vs. FCU-Split	<.001
FCU-Split	0.02 ± 0.06		
T&S	0	N/A	N/A
Smith	0	N/A	N/A
D: Coronoid surface area (cm^2)			
EMEA	3.2 ± 1.7		
		vs. Hotchkiss	.076
		vs. T&S	<.001
		vs. FCU-Split	<.001
		vs. Smith	<.001
Hotchkiss	2.3 ± 1	vs. T&S	.122
		vs. FCU-Split	.018
		vs. Smith	<.001
T&S	1.8 ± 0.9		
		vs. FCU-Split	.27
		vs. Smith	.074
FCU-Split	1.3 ± 0.7		
		vs. Smith	.289
Smith	0.9 ± 0.5		

EMEA, extended medial elbow approach; *Hotchkiss*, Hotchkiss medial over-the-top approach; *FCU-Split*, flexor carpi ulnaris splitting approach; *T&S*, Taylor and Scham approach; *N/A*, not applicable.

The EMEA showed the most coronoid surface area at 3.2 ± 1.7 cm^2 (Table ID) and proportion at 26% ± 9% (Table IID). This was followed by the Hotchkiss (20% ± 8%, $P = .076$), T&S (14% ± 5%, $P < .001$), FCU-Split (12% ± 7%, $P < .001$), and the Smith (8% ± 5%, $P < .001$) (Table IID). For coronoid height, the EMEA showed 88% ± 18% of the total height, followed by the Hotchkiss (76% ± 25%, $P = .436$), FCU-Split (61% ± 28%, $P = .058$), Smith (58% ± 35%, P = 0.034) and T&S (17% ± 10%, $P < .001$) (Table IIE). Descriptively, the EMEA, Hotchkiss, and Smith showed primarily the anterior bundle of the MCL, its insertion, and the regions anterior to it while the FCU-Split showed the anterior bundle of the MCL and regions both anterior and posterior to it. The T&S showed primarily the areas posterior to the anterior bundle of the MCL; the regions anterior to it were not visible (Fig. 6). The FCU-Split and the T&S allowed visualization of the posterior bundle of the MCL (Fig. 6).

Intraobserver reliability was excellent for all measurements, including the control distal humerus (ICC, 0.996), control coronoid (ICC, 0.986), and control radial head (ICC, 0.949). It was also excellent for the test distal humerus (ICC, 0.997), coronoid (ICC, 0.992), and radial head (ICC, 0.974). The ICCs for intraobserver reliability for the measures of proportions were 0.996, 0.998, and 0.987 for the distal humerus, coronoid, and radial head, respectively. The ICC for interobserver reliability for the control distal humerus was 0.583, 0.874 for the control coronoid, 0.41 for the control radial head, 0.915 for the test distal humerus, 0.66 for the test coronoid, and 0.583 for the test radial head. For interobserver reliability, the ICCs for the measures of proportion were 0.96, 0.663, and 0.629 for the test distal humerus, coronoid, and radial head, respectively.

Discussion

Surgical approaches to the medial side of the elbow have evolved as the indications for surgical intervention to this

Table II Proportion of joint anatomy visible

Approach	Visible	Comparison	*P* value
A: Total joint			
EMEA	15% ± 4%		
		vs. Hotchkiss	.101
		vs. FCU-Split	<.001
		vs. T&S	<.001
		vs. Smith	<.001
Hotchkiss	13% ± 3%		
		vs. FCU-Split	<.001
		vs. T&S	<.001
		vs. Smith	<.001
FCU-Split	6% ± 3%		
		vs. T&S	.091
		vs. Smith	.015
T&S	3% ± 1%		
		vs. Smith	.293
Smith	2% ± 1%		
B: Distal humerus			
EMEA	15% ± 4%		
		vs. Hotchkiss	.123
		vs. FCU-Split	<.001
		vs. T&S	<.001
		vs. Smith	<.001
Hotchkiss	13% ± 3%		
		vs. FCU-Split	<.001
		vs. T&S	<.001
		vs. Smith	<.001
FCU-Split	6% ± 2%		
		vs. T&S	.007
		vs. Smith	.004
T&S	2% ± 1%		
		vs. Smith	.760
Smith	2% ± 1%		
C: Radial head			
Hotchkiss	7% ± 3%		
		vs. EMEA	<.887
		vs. FCU-Split	<.001
EMEA	7% ± 2%		
		vs. FCU-Split	<.001
FCU-Split	0.2% ± 1%		
T&S	0	N/A	N/A
Smith	0	N/A	N/A
D: Coronoid			
EMEA	26% ± 9%		
		vs. Hotchkiss	.076
		vs. T&S	<.001
		vs. FCU-Split	<.001
		vs. Smith	<.001
Hotchkiss	20% ± 8%	vs. T&S	.122
		vs. FCU-Split	.018
		vs. Smith	<.001
T&S	14% ± 5%		
		vs. FCU-Split	.27
		vs. Smith	.074
FCU-Split	12% ± 7%		
		vs. Smith	.289
Smith	8% ± 5%		
E: Coronoid height			
EMEA	88% ± 18%		
		Hotchkiss	.436
		FCU-Split	.058
		Smith	.034
		T&S	<.001
Hotchkiss	76% ± 25%		
		FCU-Split	.365
		Smith	.287
		T&S	<.001
FCU-Split	61% ± 28%		
		Smith	.772
		T&S	<.001
Smith	58% ± 35%		
		T&S	.002
T&S	17% ± 10%		

(*continued on next column*)

(*continued*)

EMEA, extended medial elbow approach; *Hotchkiss*, Hotchkiss medial over-the-top approach; *FCU-Split*, flexor carpi ulnaris splitting approach; *T&S*, Taylor and Scham approach; *N/A*, not applicable.

area have broadened. Therefore, the purpose of this study was to assess the visible surface area of the elbow joint using laser surface scanning after 5 commonly used surgical approaches to the medial elbow. Although both Huh et al[4] and Jost et al[5] compared the surface area visible and described the access to key anatomic landmarks of the proximal ulna, MCL, and radial head, each study only compared 2 approaches and neither addressed visualization of the distal humerus, which is important in the situations where visualization of the ulnotrochlear joint is necessary. The comparison of 5 common approaches to the medial elbow, determination of the visualization of the distal humerus, and the use of a highly accurate laser surface scanning system further builds on the work previously published by both Jost and Huh.

The results of this study with respect to the coronoid are descriptively similar to those of Huh et al. Both the FCU-Split and the Hotchkiss approaches showed the anteromedial facet of the coronoid, and the FCU-Split and the Smith muscle-splitting approach exposed the sublime tubercle whereas the Hotchkiss did not.[4] The results differed as this present study found greater exposure of the coronoid with the Hotchkiss approach. This could be due to differences in technique. As mentioned, the FCU-Split approach has no standardized description in the literature, and the original description of the Hotchkiss approach can be interpreted in various ways. However, the key message is that the Hotchkiss approaches more anteriorly with little or no exposure of the sublime tubercle, whereas the FCU-Split approaches more posteriorly, giving better visualization of

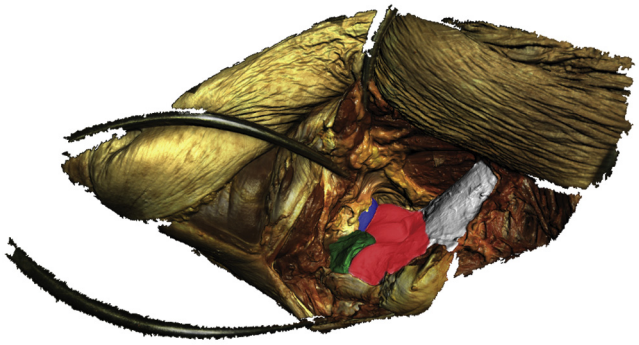

Figure 5 Extended medial elbow approach total joint area. *Red:* distal humerus surface area visualization; *green:* coronoid surface area visualization; *blue:* radial head surface area visualization.

the sublime tubercle. This study also descriptively showed that the T&S approach provides good exposure of the sublime tubercle.

In contrast to Jost et al, the present study found a significant difference in surface area visualized between the FCU-Split and the EMEA.[5] Furthermore, this current study did not reproduce visualization of posteriorly based structures through the EMEA approach, like the posterior bundle of the MCL or sublime tubercle. One reason may be that the ulnar nerve, while retracted with the FPM, was not transposed from the cubital tunnel, limiting visualization. Ulnar nerve transposition was not included in the original description of the approach, so this was not performed. Visualization of the posterior structures likely would have been possible with transposition, which can be added in the clinical setting. For the differences in surface area, one cause could be that Jost et al looked at the total ulnar surface area visualized, whereas this study only looked at the surface area of the coronoid. In their study, Jost et al did not find a difference in their order or approach, so that is likely not a factor. This study did, however, agree with Jost et al that the posterior structures were more accessible through the FCU-Split.

Finally, with respect to the descriptive analysis of the anatomical landmarks, the FCU-Split and T&S approaches routinely allowed visualization of structures posterior to the anterior bundle of the MCL. By contrast, the EMEA and Hotchkiss approaches showed more anterior structures while the structures posterior to the anterior bundle of the MCL were not visible. However, for the structures anterior to the anterior bundle of the MCL, the EMEA and the Hotchkiss were widely extensile, with both allowing visualization of the coronoid and distal humerus and across laterally to see parts of the radial head.

The strengths of this study include the analysis of several common approaches with a laser surface scanning system and internal controls, leading to a broad scope, high accuracy, and reproducibility. In contrast to previous studies[4,5] that measured visible surface area using standardized digital photographs analyzed by a computer program, the use of the laser surface scanning system was designed to improve accuracy by allowing micrometer accuracy of surface area measurements. This method was previously used by Desloges et al to measure the visible surface area of the radial head through lateral elbow approaches.[2] The limitations were that, as a cadaveric study, the results cannot fully be extrapolated to the clinical setting. With a high average cadaveric age and a female preponderance, the soft tissue bulk is likely less than what would be encountered in the clinical setting, and the exposure seen through these approaches may be greater than what can be achieved in younger, bulkier arms. Unfortunately, the number of cadavers and their demographics were limited by funding to purchase the cadavers and their availability. Furthermore,

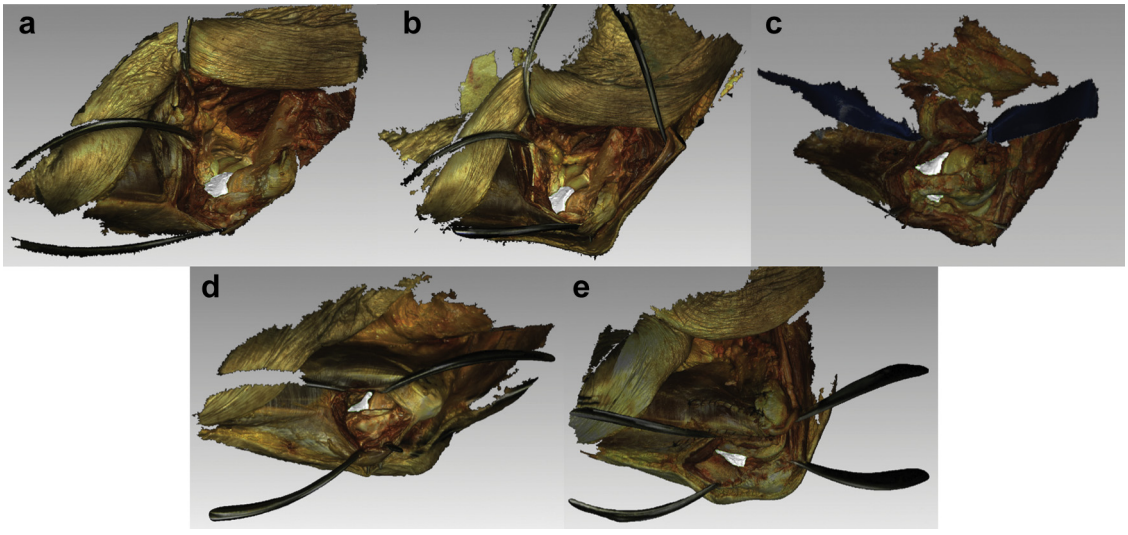

Figure 6 Coronoid visualization. (**a**) Extended medial elbow approach; (**b**) Hotchkiss medial over-the-top approach; (**c**) flexor carpi ulnaris splitting approach; (**d**) Smith approach; (**e**) Taylor and Scham approach.

several approaches were performed on each cadaver. However, steps were taken to prevent interference by standardizing the order of approaches. This particular order of approach was chosen as it started from the least invasive to the most invasive with great care taken to preserve noninvolved tissues. A similar principle was followed by starting with the most anterior approaches and moving posteriorly. The intervals were sutured closed after each approach to preserve the normal anatomy in so far as possible. It was not assessed in this study whether a different order of approaches would have altered the results; however, previous studies found no differences based on order of approach.[2,5] Furthermore, having several approaches performed on the same cadaver allowed for a repeated measures statistical analysis that is beneficial in increasing the power and decreasing the required sample size.

Finally, segmentation is user dependent and can lead to varying results. The intraobserver reliability was excellent; however, the interobserver reliability showed some heterogeneity, especially for the radial head. This can be attributed to low sample size for interobserver reliability and the difficulty in the laser scanner to delineate the radial head from the medial side. Importantly, the absolute values of the differences were low and the interobserver correlation for proportion of joint visible was in the ''good'' range, reflecting that what was clinically visible was consistent among observers.

Conclusion

The extended medial elbow approach provides the most visualization of the coronoid and distal humerus, whereas the Hotchkiss medial over-the-top approach showed the most radial head. However, these approaches mainly visualize structures anterior to the MCL. If exposure of structures posterior to the MCL is required, the floor of the ulnar nerve or Taylor and Scham approaches are more appropriate.

Acknowledgment

The authors thank Robert Potra for assistance in the creation of figures.

Disclaimer

The authors, their immediate families, and any research foundations with which they are affiliated have not received any financial payments or other benefits from any commercial entity related to the subject of this article.

References

1. Cicchetti DV, Sparrow SA. Developing criteria for establishing interrater reliability of specific items: applications to assessment of adaptive behavior. Am J Ment Defic 1981;86:127-37.
2. Desloges W, Louati H, Papp SR, Pollock JW. Objective analysis of lateral elbow exposure with the extensor digitorum communis split compared with the Kocher interval. J Bone Joint Surg 2014;96:387-93. https://doi.org/10.2106/JBJS.M.00001
3. Hotchkiss RN, Kasparyan GN. The medial ''over the top'' approach to the elbow. Tech Orthop 2000;15:105-12.
4. Huh J, Krueger CA, Medvecky MJ, Hsu JR, Skeletal Trauma Research Consortium. Medial elbow exposure for coronoid fractures: FCU-split versus over-the-top. J Orthop Trauma 2013;27:730-4. https://doi.org/10.1097/BOT.0b013e31828ba91c
5. Jost B, Benninger E, Erhardt JB, Kulling FA, Zdravkovic V, Spross C. The extended medial elbow approach-a cadaveric study. J Shoulder Elbow Surg 2015;24:1074-80. https://doi.org/10.1016/j.jse.2015.03.013
6. King GJW. Superficial Surgical Approaches of the Elbow. Tech Shoulder Elbow Surg 2002;3:2-5. https://doi.org/10.1097/00132589-200203000-00002
7. Matzon JL, Widmer BJ, Draganich LF, Mass DP, Phillips CS. Anatomy of the coronoid process. J Hand Surg Am 2006;31:1272-8. https://doi.org/10.1016/j.jhsa.2006.05.010
8. O'Driscoll SW, Jupiter JB, Cohen MS, Ring D, McKee MD. Difficult elbow fractures: pearls and pitfalls. In: Ferlic DC, editor. Instructional course lectures. Rosemont, IL: American Academy of Orthopaedic Surgeons; 2003. p. 113-34. ISBN: 978-0-89-203273.
9. Ring D, Doornberg JN. Fracture of the anteromedial facet of the coronoid process: surgical technique. JBJS Essent Surg Tech 2007;os-89(Suppl 2):267-83. https://doi.org/10.2106/JBJS.G.00059
10. Shrout PE, Fleiss JL. Intraclass correlations: uses in assessing rater reliability. Psychol Bull 1979;86:420-8.
11. Smith GR, Altchek DW, Pagnani MJ, Keeley JR. A muscle-splitting approach to the ulnar collateral ligament of the elbow. Neuroanatomy and operative technique. Am J Sports Med 1996;24:575-80.
12. Steinmann SP. Coronoid process fracture. J Am Acad Orthop Surg 2008;16:519. https://doi.org/10.5435/00124635-200808000-00013
13. Taylor TK, Scham SM. A posteromedial approach to the proximal end of the ulna for the internal fixation of olecranon fractures. J Trauma 1969;9:594-602.